

Article

Primary Atmospheric Oxidation Mechanism for Toluene

Cristian O. Baltaretu, Eben I. Lichtman, Amelia B. Hadler, and Matthew J. Elrod

J. Phys. Chem. A, **2009**, 113 (1), 221-230 • Publication Date (Web): 15 December 2008

Downloaded from <http://pubs.acs.org> on January 22, 2009

More About This Article

Additional resources and features associated with this article are available within the HTML version:

- Supporting Information
- Access to high resolution figures
- Links to articles and content related to this article
- Copyright permission to reproduce figures and/or text from this article

[View the Full Text HTML](#)

Primary Atmospheric Oxidation Mechanism for Toluene

Cristian O. Baltaretu, Eben I. Lichtman, Amelia B. Hadler, and Matthew J. Elrod*

Department of Chemistry and Biochemistry, Oberlin College, Oberlin, Ohio 44074

Received: July 31, 2008; Revised Manuscript Received: September 25, 2008

The products of the primary OH-initiated oxidation of toluene were investigated using the turbulent flow chemical ionization mass spectrometry technique at temperatures ranging from 228 to 298 K. A major dienedial-producing pathway was detected for the first time for toluene oxidation, and glyoxal and methylglyoxal were found to be minor primary oxidation products. The results suggest that secondary oxidation processes involving dienedial and epoxide primary products are likely responsible for previous observations of glyoxal and methylglyoxal products from toluene oxidation. Because the dienedial-producing pathway is a null cycle for tropospheric ozone production and glyoxal and methylglyoxal are important secondary organic aerosol precursors, these new findings have important implications for the modeling of toluene oxidation in the atmosphere.

Introduction

Aromatic compounds are an important class of hydrocarbons—particularly in urban environments—in the formation of both tropospheric ozone and aerosols. In the United States, automobile emissions are the dominant source of aromatic compounds, with significant emissions also resulting from their use as solvents in various manufacturing processes.¹ Measurements made in Boston indicate that aromatic compounds make up about 30% of the total nonmethane hydrocarbon (NMHC) content of the atmosphere, and are responsible for about 40% of the ozone producing potential of all NMHCs.² The most abundant aromatic compounds are usually benzene, toluene, dimethylbenzenes (xylenes), ethylbenzene, and trimethylbenzenes. Aromatic compounds have also been implicated as source compounds in the formation of secondary organic aerosol (SOA), with toluene having received the most detailed study.^{2,3} Thus, an understanding of the role of aromatic compounds in air pollution is essential to the overall effort to improve air quality.

Despite an intense effort to understand the photochemical oxidation mechanisms for the important aromatic compound class, there remain a number of key uncertainties. A recent study stated: "...photochemistry of this class of compounds [aromatics] is very poorly understood and the chemistry implemented in the toluene mechanism is very speculative."⁴ In particular, the existing mechanisms overpredict the amount of ozone produced, underpredict the extent of radical chemistry, and cannot account for the NO_x sensitivity of environmental chamber experiments.⁴ Several experimental studies are also in conflict concerning the number of oxidation cycles required to produce SOA precursors. These outstanding issues are important as they directly hinder the ability to model the contributions of aromatic compounds to the problem of air pollution, and thus, the effort to construct effective regulatory policies to improve air quality.

As the result of three decades of study, it is now known that the atmospheric oxidation of aromatic compounds proceeds through a variety of complex reactions. For the purposes of this discussion, *primary oxidation* will refer to any oxidation sequence initiated by a single OH attack on the precursor

aromatic hydrocarbon; *secondary oxidation* will refer to any oxidation sequence initiated by a single OH attack on the *product* of a primary oxidation reaction. Figure 1 synthesizes many of the previously proposed mechanisms for the *primary oxidation* of aromatic compounds, but it is primarily based upon the scheme proposed by Calvert et al.² The compounds enclosed by boxes in Figure 1 have been observed as stable oxidation products in at least one experimental study. The species in Figure 1 are labeled according to a scheme that indicates whether only O₂ chemistry is needed (label: O2), or whether NO chemistry is also needed (label: NO) to produce the particular compound. The number in the label refers to the total number of bimolecular reaction steps in the primary oxidation sequence required to produce the species from the aromatic precursor, and the letter identifies each unique chemical species. For example, the species in the lower right side of Figure 1 labeled NO4a, requires both O₂ and NO chemistry, and a total of four bimolecular reaction steps are required to transform the aromatic precursor into species NO4a.

The initial OH attack on toluene can occur via two mechanisms: H-atom abstraction from the methyl group and OH-addition to the aromatic ring. The H-atom abstraction route goes through the usual peroxy intermediate (O2j in Figure 1) which then undergoes reaction with HO₂ (or NO) to ultimately form the stable benzaldehyde product (HO2a). The latest master chemical mechanism (MCM) treatment for toluene oxidation separates the OH-addition route into three general categories according to the type of product eventually produced: (1) phenol (O2i), (2) epoxide (O3c), and (3) peroxy-bicyclic ring-opening (butenedial NO4c-2 and glyoxal NO5).⁵ These categories implicitly indicate the importance of the intermediates O1b, O2b, and O3b, respectively, in leading to the three categories of products.

However, there are several uncertainties in the mechanism given in Figure 1. For example, the MCM model does not explicitly deal with the dienedial product O2h, which, according to Figure 1, can be produced with or without NO chemistry. In almost all pathways, HO₂ is produced, which, through its role in converting NO to NO₂, is the key player in the ability of aromatic compounds to contribute to ground level ozone formation. However, the formation of a dienedial

* Corresponding author. E-mail: mjelrod@oberlin.edu.

processes are generally operative in aromatic oxidation systems (and for toluene, specifically).

There is also uncertainty concerning the role of primary vs secondary oxidation processes in producing the observed oxidation products. Klotz et al.⁶ have suggested that the dienial product (O2h) could undergo secondary oxidation to produce the observed products butenedial (NO4c-2) and glyoxal (NO5a). The ambiguity concerning whether these species are the products of primary or secondary oxidation events is related to the fact that most experiments continuously produce OH in the reaction system. In addition, most experimental methods use a photochemical OH source, which leaves open the possibility of the photochemical degradation of products such as the dienial species, as well. On the other hand, there is competing kinetic evidence that glyoxal is in fact a primary oxidation product.⁷ In any case, the importance of determining whether glyoxal is a primary or secondary oxidation product is 2-fold. In addition to the potential of differing overall rates depending on whether the primary or secondary oxidation process is operative and the corresponding effect on ozone production, the kinetics of glyoxal formation is also relevant to glyoxal's role as an SOA precursor.⁸ For the purposes of understanding SOA formation from aromatics in general, it is important to understand how many oxidation events are necessary to create SOA precursors. For toluene, both primary oxidation products (benzaldehyde and phenols) and secondary oxidation products (diols and quinones formed from phenols and benzoic acid formed from benzaldehyde) have been identified in SOAs (among a complex array of other compounds).^{9,10} Therefore, it is of interest to use experimental methods in which the primary and secondary oxidation chemistry can be more tightly controlled, in order to allow the primary and secondary steps to be definitively identified.

The role of NO in the aromatic oxidation mechanisms has also been difficult to determine in part due to the experimental conditions most commonly used. In most of these experiments, OH itself was generated via photochemical reactions involving NO, and it was not possible to definitively identify products arising specifically from NO reactions. However, it is clear that NO chemistry plays a significant role in the conditions used by most previous workers. For example, Klotz et al.¹¹ showed that in the oxidation of benzene, the phenol yields drop in the presence of elevated NO. Berndt and Boge¹² also found that the phenol yields from benzene oxidation drop in the presence of elevated NO, and that the dienial yields increase. Consequently, it is desirable to apply experimental methods in which the NO levels can be varied independently of the OH levels, with NO-free experiments being of particular interest.

Finally, there is currently very poor agreement among existing product yield measurements for toluene at 298 K,^{7,13–25} and there has been only one temperature dependent study²⁶ (at temperatures higher than 298 K). There have been a wide variety of products detected using the various experimental methods formed from the oxidation of toluene. However, the H-abstraction product (benzaldehyde), phenol, glyoxal, and methyl glyoxal were most often detected. The epoxide species (O3c) included in the MCM model has been tentatively detected in only one instance for the toluene system.²⁷ Interestingly, a dienial product has not yet been quantified for the toluene oxidation system (a dienial product has previously been observed in the benzene oxidation system^{11,12}). With the exception of the benzaldehyde product yield for toluene, the quantitative agreement of the various benzene and toluene oxidation studies is quite poor. Of course, the potential problems discussed above concerning the possible role of secondary

oxidation chemistry and the role of NO are likely explanations for at least some portion of the poor agreement between the various studies. In particular, the yields of glyoxal and methylglyoxal products from toluene oxidation in the different experiments are strikingly different, with the range of values extending from 3.7 to 39%. These discrepancies could potentially be explained by a strong NO-dependent effect in a primary oxidation sequence, or by the role of secondary oxidation in the production of glyoxal and methylglyoxal products. It is also possible that there are detection biases in some of the previous work, as most of the experimental approaches have used either GC-MS or FT-IR detection techniques. The GC-based method may be unreliable for such potentially thermally unstable species as the dienial product, and the IR approaches have difficulty distinguishing between different carbonyl containing compounds. In addition, there are very few experiments in which most important oxidation products have been simultaneously measured, and there are no quantitative estimates at all for dienial for the toluene oxidation system. Therefore, it is of interest to apply experimental methods in which many of the important oxidation products can be simultaneously observed.

This article describes the identification of primary oxidation system intermediates and the detection and quantification of stable primary oxidation products over the temperature range 228–298 K for toluene via the turbulent flow chemical ionization mass spectrometry (TF-CIMS) technique. In particular, the CIMS approach allowed for a more complete identification of the reaction system species, and the TF method provided the facility to separately control OH and NO levels in the system, as well as the ability to perform temperature dependence studies of relevance to the entire troposphere.

Experimental Section

Turbulent Fast Flow Tube. A schematic of the experimental apparatus is given in Figure 2, and is similar to that described by Miller et al. in their study of the overall reaction rate of alkene-derived hydroxyperoxy radicals with NO.²⁸ The main flow tube was 100 cm in length and constructed with 2.2 cm inner diameter Pyrex tubing. A large flow of nitrogen carrier gas (30 STP L min⁻¹) was introduced at the rear of the flow tube to serve as the bulk flow gas. The reactants necessary for the production of OH radicals were also introduced at the rear of the flow tube through a 20 cm long, 12.5 cm inner diameter sidearm. In most experiments, the aromatic precursors and O₂ were added to the sidearm immediately downstream of the OH source, as shown in Figure 2. In other experiments, the aromatic precursors and O₂ were added to the rear of the flow tube, at the same injection point as the N₂ carrier gas. For experiments involving NO or OH radical scavengers, these gases were introduced into the main flow tube through an encased moveable injector. The encasement was made of corrugated Teflon tubing and allowed the injector to be moved to various injector positions ("time = zero" injector position is set just upstream of the ionization source) without breaking any vacuum seals. A fan-shaped Teflon device was placed at the end of the injector to enhance turbulent mixing. All gas flows were monitored with calibrated mass flow meters. A polonium-210 (²¹⁰Po) α -particle-emitting ionization source was placed between the flow tube and the entrance to the CIMS. Flow tube pressure and temperature were measured upstream of the ionization source. Pressure was measured using a 0–1000 Torr capacitance manometer. Temperature was determined using Cu–constantan thermocouples. Most of the flow tube gases were removed at the CIMS inlet using a 31 L s⁻¹ roughing pump.

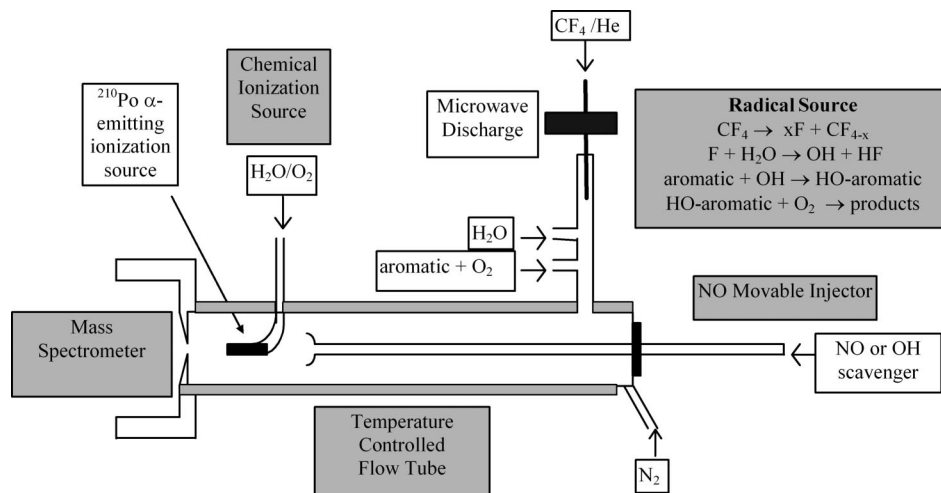
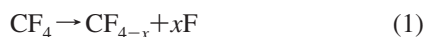


Figure 2. Experimental apparatus.

For the low temperature studies, liquid nitrogen cooled silicone oil was used as the coolant for the jacketed flow tube. Nitrogen carrier gas was precooled by passing it through a copper coil immersed in a liquid N₂ reservoir followed by resistive heating. The temperature was controlled in the reaction region to within ± 1 K.

The pressure was maintained at 100 ± 1 Torr in order to achieve optimum instrument performance. Pressures below 100 Torr were found to lower the ionization efficiency and pressures above 100 Torr were found to lower the radical production efficiency.

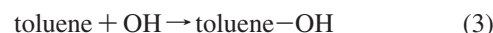
OH Source. The OH radical species were generated using the microwave discharge technique to produce F atoms, followed by reaction with H₂O:



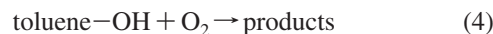
A dilute mixture of He/CF₄ was passed through a microwave discharge, produced by a Beenakker cavity operating at 50 W, to create fluorine atoms (reaction 1). The dilute mixture was obtained by combining a 5.0 STP L min⁻¹ flow of ultrahigh purity helium (99.999%) with a 1.0 STP mL min⁻¹ flow of a 2% CF₄ (99.9%)/He mixture. The 5.0 STP L min⁻¹ helium flow was first passed through a silica gel trap immersed in liquid nitrogen to remove any possible impurities. The fluorine atoms were then injected into the flow tube sidearm and mixed with H₂O/He, produced by bubbling 10.0 mL min⁻¹ He through a trap filled with H₂O to produce OH radicals (reaction 2). Because H₂O is in great excess ($[\text{H}_2\text{O}] = 2 \times 10^{14}$ molecule cm⁻³) and the F + H₂O reaction is very fast (1.4×10^{-11} cm³ molecule⁻¹ s⁻²),²⁹ the OH-producing reaction has a very short lifetime of about 0.4 ms, thus ensuring that all F atoms are quickly consumed. It is also useful to estimate the approximate concentration of OH produced by the radical source. Absolute OH concentrations (in the absence of aromatic precursors) were determined by titrating OH with NO₂ to produce HNO₃. The absolute HNO₃ concentrations were determined by the calibration of the HNO₃ mass spectrometer signal using a bubbler containing 60% HNO₃ solution by weight, immersed in an ice-water bath. The vapor pressure of HNO₃ for this solution at 273 K is 0.20 Torr.³⁰

Primary Oxidation Product Studies. In most experiments, toluene (or, one of its deuterium-substituted isotopes, C₆H₅CD₃ or C₇D₈) and O₂ were added to the sidearm where OH was

produced. The typical sidearm concentrations for these experiments were $[\text{toluene}] = 3.5 \times 10^{13}$ and $[\text{O}_2] = 6 \times 10^{16}$ molecule cm⁻³. Using the known OH + toluene rate constant of about 6×10^{-12} cm³ molecule⁻¹ s⁻¹,²⁹ OH has a lifetime of about 5 ms under these conditions to produce the toluene-OH adduct:



Using the estimated rate constant for the reaction of the toluene-OH adduct with O₂ of 3×10^{-15} cm³ molecule⁻¹ s⁻¹,³¹ the toluene-OH adduct lifetime is about 6 ms under these conditions and this reaction leads to the products depicted in Figure 1:



Because the residence time of gases in the sidearm is about 40 ms, both the toluene + OH and toluene-OH + O₂ reactions are expected to be complete before the various species enter the main flow tube.

In other experiments, toluene and O₂ were added to the main flow tube. Because of the dilution effect of the large N₂ main flow, the concentrations of all species were seven times smaller than those present in the sidearm experiments.

NO Dependence Studies. NO [$\sim 1 \times 10^{13}$ molecule cm⁻³] was introduced into the main flow tube as a 2% NO/N₂ mixture through the moveable injector or into the sidearm at the same injection point as toluene and O₂. The mixture was first passed through a silica gel trap held between -20 and -30 °C to remove any traces of NO₂ impurities. Negligible amounts of NO₂ impurities were observed using the CIMS technique.

OH Scavenger Studies. 1-butene [$\sim 3 \times 10^{13}$ molecule cm⁻³], which is known to efficiently form peroxy radicals in the presence of OH and O₂,²⁸ was introduced to the main flow tube as a 10% 1-butene/N₂ mixture through the moveable injector. Although the concentrations of 1-butene and toluene are similar in this experiment, the OH + 1-butene reaction has a rate constant that is about 5 times larger than that of the OH + toluene reaction. Therefore, the 1-butene species outcompetes toluene for OH under these conditions.

CIMS Detection. The chemical ionization reagent ions were produced using a commercial polonium-210 α -particle emitting ionization source consisting of a hollow cylindrical (69 by 12.7 mm) aluminum body with 10 mCi (3.7×10^8 disintegrations s⁻¹) of polonium-210 coated on the interior walls. All oxygen-

ated organic species were detected using a proton transfer CIMS scheme. The $\text{H}^+(\text{H}_2\text{O})_n$ ions were produced by passing a large O_2 flow (7 STP L min^{-1}) through the ionization source with H_2O impurities being sufficiently abundant to produce an adequate amount of reagent ions. The predominant species detected were the protonated (and partially hydrated) analogs of the neutral precursor oxygenated organic compounds. No fragment ions were detected. Toluene was detected with a C_4H_9^+ -adduct forming CIMS scheme. C_4H_9^+ reagent ions were produced by combining a large flow of N_2 (7 STP L min^{-1}) with a 12 STP mL min^{-1} flow of isobutane and passing the mixture through the ionization source. The predominant species detected was $\text{C}_7\text{H}_8\text{--C}_4\text{H}_9^+$. A negative ion CIMS scheme was used to the presence of NO_2 . SF_6^- reagent ions were produced by combining a large flow of N_2 (7 STP L min^{-1}) with a 1.5 STP mL min^{-1} flow of 10% SF_6/N_2 and passing the mixture through the ionization source. The predominant species detected were NO_2^- and $\text{H}_2\text{O NO}_2^-$. Ions were detected with a quadrupole mass spectrometer housed in a two-stage differentially pumped vacuum chamber. Flow tube gases (neutrals and ions) were drawn into the front chamber through a charged 0.1 mm aperture. The front chamber was pumped by a 6 in. 2400 L s^{-1} diffusion pump. The ions were focused by three lenses constructed from 3.8 cm inner diameter and 4.8 cm outer diameter aluminum gaskets, and then entered the rear chamber through a skimmer cone with a charged 1.0 mm orifice. The skimmer cone was placed approximately 5 cm from the front aperture. The rear chamber was pumped by a 250 L s^{-1} turbomolecular pump. After the ions had passed through the skimmer cone, they were mass filtered and detected with a quadrupole mass spectrometer.

Relative Product Yield Studies. The relative product yield is defined as the flow tube concentration of the species of interest divided by the sum of the flow tube concentrations of all measured products. As discussed in the results section, the CIMS technique allows for the identification of four major reaction products from the primary oxidation of toluene: benzaldehyde, cresol, dienedial, and epoxide. For example, the relative yield % equation for benzaldehyde is defined as follows:

$$\text{relative yield \% benzaldehyde} = \frac{[\text{benzaldehyde}]}{[\text{benzaldehyde}] + [\text{cresol}] + [\text{dienenial}] + [\text{epoxide}]} \times 100 \quad (5)$$

This quantity requires the absolute concentrations of all four product species to be determined. Calibration curves for authentic samples of benzaldehyde and *o*-cresol were constructed by flowing a known concentration of each substance into the flow tube, and measuring the CIMS response.

Since a mixture of *o*-, *m*-, and *p*-cresol is actually being generated in the oxidation system, there is a potential complication if the CIMS response for *m*- and *p*-cresol are different from that of *o*-cresol, the calibration standard. The CIMS response for the proton transfer detection of these species is largely determined by the ion molecule rate constant for the reaction of the neutral species with H_3O^+ . In the case of oxygenated compounds—because the electronegative oxygen atom is the target of the proton transfer process—the rate constants tend to be similar for compounds with identical oxygen-containing functional groups. For example, in one study,³² methanol, ethanol, 1-propanol, 1-butanol and phenol were all found to have the same H_3O^+ ion–molecule rate constant of $2.7 \times 10^{-9} \text{ cm}^3 \text{ s}^{-1}$. Therefore, no significant difference in CIMS response is expected among the aromatic alcohols (*o*-, *m*-, and *p*-cresol)

measured in this work. However, as a spot check, the CIMS response for *o*- and *p*-cresol was compared and found to be identical within the error limits of the calibration method ($\pm 20\%$).

Because authentic samples for the dienedial and epoxide products are not available, a proxy standard was used. In the case of the dienedial, because both oxygen-containing functional groups are aldehydes, it is expected that the H_3O^+ ion–molecule rate constants will be similar to other aldehydes. Previous measurements have indicated that the H_3O^+ ion–molecule rate constants for butanal, heptanal, octanal, and decanal are virtually identical,³³ ranging only from 3.7×10^{-9} to $3.9 \times 10^{-9} \text{ cm}^3 \text{ s}^{-1}$. Apparently, there is only one experimental measurement of the H_3O^+ ion–molecule rate constant for a dial—that for pentanedial,³⁴ which was found to have a rate constant of $3.9 \times 10^{-9} \text{ cm}^3 \text{ s}^{-1}$, a value that is similar to those reported above for the simple aldehydes. Therefore, octanal was adopted as the proxy standard for the dienedial, as it appears that aldehydes and dials can be assumed to have similar H_3O^+ ion–molecule rate constants and thus are expected to have similar CIMS responses. If the H_3O^+ ion–molecule rate constants for the dienedial and the epoxide are significantly different than octanal, the errors introduced into the product yield measurements are expected to scale linearly with the relative difference in the rate constants as compared to octanal. Since these rate constants are near the collision limit, any systematic errors of this kind are more likely to lead to underestimates of the dienedial yields. Octanal was specifically selected as the proxy standard because it has a convenient vapor pressure for the generation of calibration data over the appropriate concentration range.

The selection of a proxy standard for the epoxide is more complicated. Since the epoxide species also has two aldehyde functional groups, it is not immediately obvious whether an epoxide or aldehyde proxy standard would be most appropriate. In these cases, the proton affinity for protonation at the different oxygen-atom sites can be used to predict the site of the proton-transfer event. High level electronic structure calculations (M2G2MS) were performed (to be described in detail in future work) on the epoxide species to determine the proton affinity for protonation at the epoxide oxygen atom, the aldehyde oxygen atom at the 1-position, and the aldehyde oxygen atom at the 6 position. The proton affinities for the two aldehyde oxygen atoms were found to be 793 and 795 kJ mol^{-1} , respectively. The proton affinity for the epoxide oxygen atom was found to be 747 kJ mol^{-1} . The uncertainty in proton affinity values at the M2G2MS level of theory has been previously estimated³⁵ to be about 10 kJ mol^{-1} . Therefore, the proton transfer process is expected to take place at either of the aldehyde oxygen atoms, and the CIMS response for the epoxide species is expected to be similar to other aldehydes. For this reason, octanal was again chosen as proxy standard for the epoxide species. The yields of the potential products, glyoxal, methylglyoxal, and butenedial (all with dial functionality), were also estimated using octanal as a proxy CIMS calibration standard.

Absolute Product Yield Studies. The absolute product yield is defined as the flow tube concentration of the species of interest divided by the total amount of reacted toluene precursor. The latter quantity can be determined by measuring the difference in the toluene flow tube concentrations with the OH source on and off. Since the toluene concentrations for the conditions with the OH source off are simply calculated from the flow conditions, the amount of reacted toluene precursor is simply calculated from the ratio of the CIMS signal for the two condi-

TABLE 1: Correspondence Between Observed Ions and C₆H₅CD₃ Oxidation Products

ion	<i>m/z</i> (amu)			
	benzaldehyde (HO ₂ a) (C ₇ H ₅ DO)	cresol (O ₂ i) (C ₇ H ₅ D ₃ O)	dienedial (O ₂ h) (C ₇ H ₅ D ₃ O ₂)	epoxide (O ₃ c) (C ₇ H ₅ D ₃ O ₃)
H ⁺	108	112	128	144
H ⁺ (H ₂ O)	126	130	146	162

tions, multiplied by the OH source off toluene flow tube concentration:

$$[\text{reacted toluene}] = \frac{(\text{toluene CIMS signal})_{\text{OH source on}}}{(\text{toluene CIMS signal})_{\text{OH source off}}} \times [\text{toluene}]_{\text{OH source off}} \quad (6)$$

For example, the absolute yield % equation for benzaldehyde is defined as follows:

$$\text{absolute yield \% benzaldehyde} = \frac{[\text{benzaldehyde}]}{[\text{reacted toluene}]} \times 100 \quad (7)$$

Results and Discussion

Primary Product Identification. In the NO-free experiments, four major products from the primary oxidation of toluene were identified based on CIMS spectra collected for OH + C₇H₈, OH + C₆H₅CD₃, and OH + C₇D₈. The OH + C₆H₅CD₃ experiments were particularly useful, as the four products each have unique *m/z* ratios in the proton transfer chemical ionization mass spectrum. The four products were identified according to the correspondence between the protonated (and in some cases, also hydrated) ions and the neutral oxidation products (general product family names, specific formulas for C₆H₅CD₃ oxidation products are given in Table 1). The observation of a dienedial major product for toluene is an important finding, and the observation of the epoxide product is only the second such measurement for the toluene system.²⁷

In order to confirm that the observed product distribution was predominantly the result of primary oxidation of toluene by OH, two additional experiments were performed. In one experiment, very high sidearm concentrations of toluene were used (3×10^{14} molecule cm⁻³). If some OH were reacting with primary oxidation products at the lower toluene concentration (3.5×10^{13} molecule cm⁻³), the product distribution would be expected to be different under the higher toluene concentration conditions, where OH is much less likely to react with species other than toluene. The product distribution did not appreciably change as the toluene concentration was increased, indicating that the principal fate of OH in the sidearm is reaction with toluene, and not reaction with any of the primary oxidation products. In the other experiment, toluene and O₂ were added to main flow tube, thus forcing the toluene–OH–O₂ chemistry to occur in the main flow tube. Since all species in this reaction situation are at concentrations seven times smaller than the sidearm concentrations (due to the dilution effect of the carrier N₂ flow), any reactions involving products of the primary oxidation event should be slowed down. Under these more dilute conditions, the benzaldehyde product formation was suppressed by about 30%, while the cresol, dienedial, and epoxide production formation was largely unchanged. Therefore, at least some of the benzaldehyde product formation appears to be the result of secondary chemistry involving species other than OH (most likely the reaction of HO₂ with the peroxy radical species, O₂j in Figure 1, as is discussed below in the section describing the

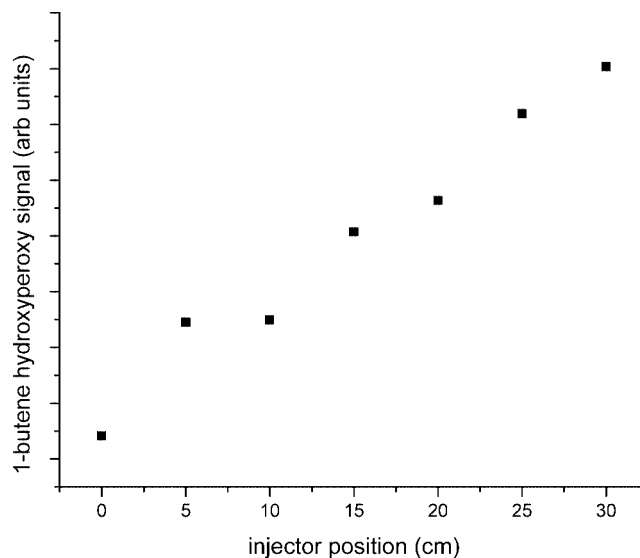


Figure 3. OH regeneration kinetics with 1-butene scavenger.

NO dependence experiments). It is worth noting that this chemistry is the result of a single OH attack on toluene; therefore, from the point of view of OH, benzaldehyde is properly categorized as a primary oxidation product.

Peroxy Radical Detection. The mechanism given in Figure 1 presumes the presence of several peroxy radical intermediates in the primary oxidation mechanism for toluene. Our past experience with organic peroxy radicals^{28,36–41} indicate that proton transfer CIMS is a general technique for the detection of these species because of the relatively high proton affinity of the peroxy functional group. In particular, past experience has shown that these organic peroxy species can be detected at about the 100 ppt level (or 3×10^9 molecules cm⁻³ at 100 Torr) with the TF-CIMS technique. Since the approximate initial OH concentrations in these experiments were determined to be no lower than 1×10^{11} molecules cm⁻³, signal-to-noise ratios for the species of interest are expected to be on the order of at least 30:1. Therefore, the proton transfer CIMS technique is expected to be capable of detecting long-lived (the maximum residence time of the flow system is about 100 ms) peroxy intermediates of the major product pathways in the primary oxidation of toluene.

A small proton transfer CIMS signal with a signal-to-noise ratio of about 5:1 attributed to a peroxy radical with the formula C₆H₅CD₂O₂ was observed in the oxidation of C₆H₅CD₃ (C₆H₅CH₂O₂ was also observed in the oxidation of C₆H₅CH₃). This species is most likely the peroxy radical intermediate (species O₂j in Figure 1) in the pathway that eventually leads to the benzaldehyde primary product, as discussed in the section above. The identification of this species as a peroxy radical was supported by its suppression in the presence of NO. However, no other peroxy species were identified, despite the fact that several of the other product channels dominate over the benzaldehyde pathway. Therefore, if peroxy radical intermediates are important in the other primary oxidation pathways, they are apparently too short-lived to be observed with the TF-CIMS technique.

OH Regeneration. Figure 1 indicates that if the dienedial product (O₂h) is formed in an NO-free environment, OH should be observed as a coproduct. Figure 3 shows the results of an experiment in which the 1-butene scavenger is introduced into the main flow tube at different injector positions (different flow tube reaction times) and the resulting 1-C₄H₈(OH)(O₂) species

is monitored. Because the OH lifetime in the sidearm is too short to allow OH from the microwave discharge source to be transported into the main flow tube, these experiments suggest that OH is being formed by the toluene oxidation system. This result, in combination with the observation of the dienedial product discussed above, suggests that the dienedial product may form via a NO-free mechanism, regenerating OH rather than the HO₂ coproduct characteristic of the other product channels or that some other intermediate decomposes to release OH.

NO Dependence. Two different NO dependence experiments were performed. In both experiments, the NO concentrations ($\sim 1 \times 10^{13}$ molecule cm⁻³) were chosen to be large enough to drive any potential peroxy + NO reaction (assuming a rate constant of 1×10^{-11} cm³ molecule⁻¹ s⁻¹)²⁸ to completion on the time scale of either the sidearm (40 ms) or main flow tube (70 ms) residence times. In one experiment, NO was added through the movable injector. In this experiment, the toluene-OH-O₂ reactions were expected to be completed by the time the relevant species encountered NO in the main flow tube (this spatial separation corresponds to a time delay of about 50 ms). In the other experiment, NO was added at the same injection point as toluene and O₂ in the sidearm. In this experiment, the toluene-OH-O₂ reactions are not spatially separated from potential NO reactions, as is the case in the first experiment. However, if the toluene-OH-O₂ chemistry is happening too quickly for any potential NO reactions to compete, there will be no difference in the products observed for the two experimental conditions. Interestingly, the proton transfer mass spectra for both of these NO experiments were very similar and differed only slightly from the NO-free mass spectra. In particular, the amount of all products is somewhat increased as a result of the presence of NO. Presumably, this is due to the conversion of the HO₂ coproduct (characteristic of several of the primary oxidation channels outlined in Figure 1) to OH,



which stimulates further oxidation of toluene, eventually leading to additional product formation. Indeed, negative mode CIMS measurements of NO₂ during these experiments confirm that the toluene oxidation system efficiently converts NO to NO₂. The benzaldehyde channel is further enhanced by the presence of NO, presumably due to the reactions



In the absence of NO, C₆H₅CH₂O is formed from the slower C₆H₅CH₂O₂ + HO₂ reaction, which apparently leads to less benzaldehyde product. Note that this invocation of secondary HO₂ chemistry is supported by the earlier observation that the benzaldehyde product yield was affected by the overall concentration of the product species.

Figure 1 indicates that the reaction between a bicyclic peroxy intermediate (O3b) and NO is the key step in the proposed primary oxidation mechanism for the production of methylglyoxal (NO5a) and butenedial (NO4c-2). Many previous studies have also reported glyoxal as a product, which presumably forms from a different isomeric form of species NO4a. In our previous work on the OH-initiated oxidation of alkynes, proton transfer CIMS methods were used to detect glyoxal (observed at *m/z* 59, 77, and 95) and methylglyoxal (observed at *m/z* 76, 94, 112) products.³⁹ Similarly, butenedial would be expected to be observed at *m/z* ratios of 85, 103, 121. For all three species, no reproducible signals were observed above the background level at the relevant *m/z* values. Therefore, it does not appear that glyoxal, methylglyoxal or butenedial are major products in the primary oxidation of toluene. However, in order to calculate specific upper limit values for the yields of these products, the total signal (i.e., the background was assumed to be zero) at each *m/z* ratio was used (in combination with the proxy CIMS standard) to determine the concentrations for each of the species. Because the background contribution is ignored in these calculations, the yields calculated from these concentrations constitute an upper limit for glyoxal (4%), methylglyoxal (4%), and butenedial (2%).

Absolute Primary Oxidation Product Yield Measurements at 298 K. The absolute primary product yields for C₆H₅CD₃ under NO-free conditions were determined by averaging the results of four independent experiments. The mean yields and statistical uncertainties from these experiments are given in Table 2 (along with the results from previous experiments). The main source of error in this measurement were the run to run variability ($\sim 20\%$) in the CIMS signal for each product and the variability in the CIMS response factor ($\sim 20\%$). The sum of the yields is somewhat less than 100%, which could be due to unquantified products or an overestimate of toluene reactivity. As discussed above, while the cresol, dienedial, and the epoxide products appear to be the result of primary OH/O₂ chemistry only, the final benzaldehyde product yield depends on both on

TABLE 2: Toluene Oxidation Product Absolute Yield Percentage Measurements

	benzaldehyde	cresol	dienedial	epoxide	glyoxal	methylglyoxal
Volkamer et al. ⁷					39	
Moschonas et al. ¹³	8.4	9.0				
Klotz et al. ¹⁴	5.8	17.9				
Smith et al. ¹⁵	6	15			23.8	16.7
Becker et al. ¹⁶	7.1				3.7	4.4
Seuwen et al. ¹⁷	5.3	52.9			4.1	5.5
Atkinson et al. ¹⁸		12.3				
Atkinson et al. ¹⁹	6.45	25.2				
Dumdei et al. ²⁰	5				27	14
Tuazon et al. ²¹					10.5	14.6
Gery et al. ²²					9.8	10.6
Bandow et al. ²³	11				15	14
Shepson et al. ²⁴	5.4				8	7.5
Tuazon et al. ²⁵					11.1	14.6
present work ^a	4.9 ± 1.8	28.1 ± 6.1	23.5 ± 8.7	7.2 ± 2.5	<4	<4

^a NO-free values.

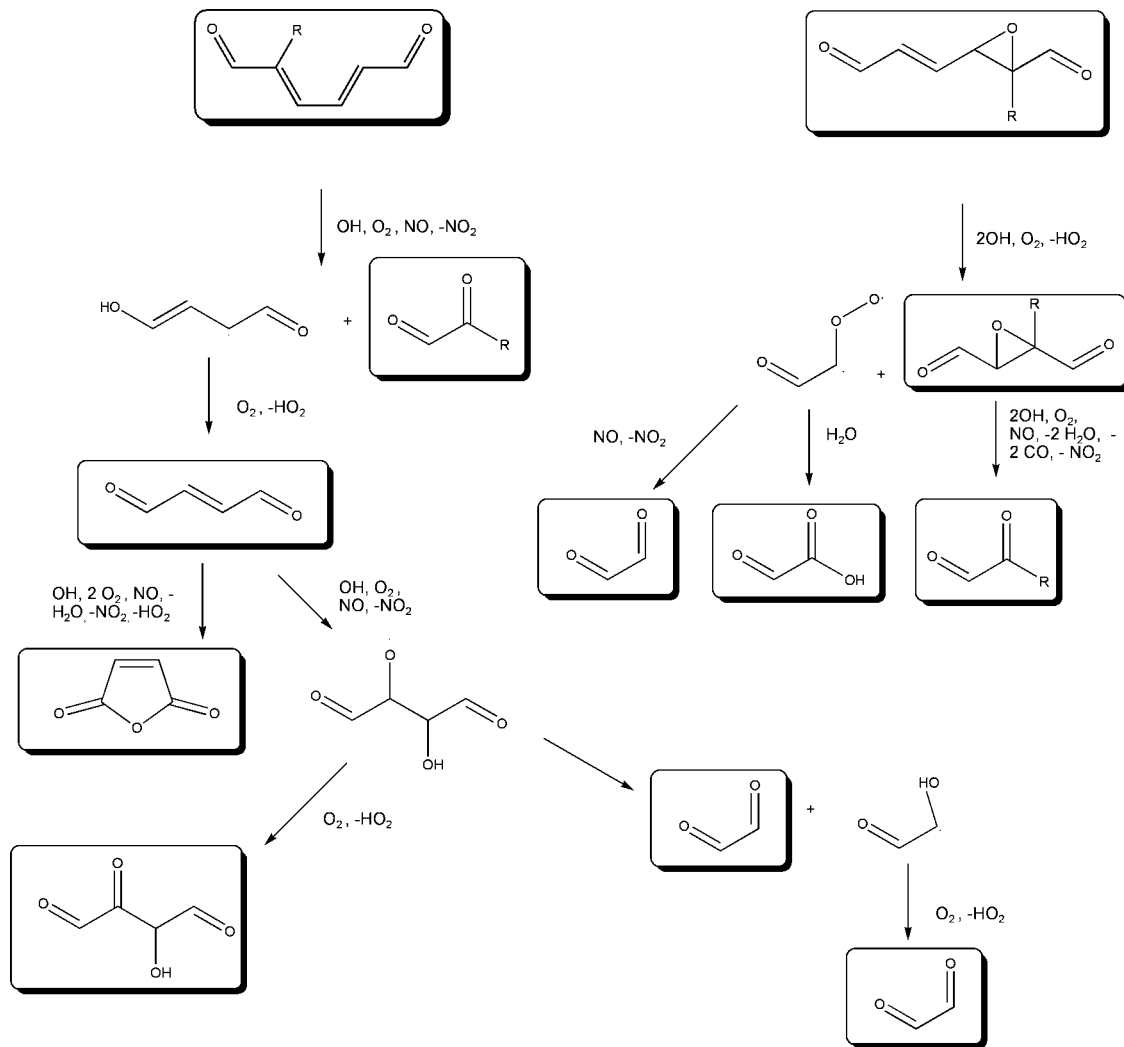


Figure 4. Postulated secondary oxidation of dienedial and epoxide primary products.

the HO₂ and NO levels in the experiment. In light of this, it is perhaps not surprising that the present NO-free yield for benzaldehyde is lower than all of the previous measurements, most of which involved the presence of NO.

However, there are two more important differences between the present results and previous results. The first difference is the observation and quantification of the dienedial and epoxide channels, which had not been previously accomplished for the toluene oxidation system. The second difference is the present finding that glyoxal and methylglyoxal are not major primary oxidation products. As discussed in the introduction, the explanations for both of these differences are likely related. Our hypothesis is that previous observations of glyoxal and methylglyoxal products in the oxidation of toluene are due to *secondary* oxidation chemistry involving the dienedial and/or epoxide primary oxidation products. In Figure 4, secondary oxidation pathways are proposed for the dienedial (primarily based on the suggestion of Klotz et al.⁶) and the epoxide (based on the standard OH-initiated oxidation mechanism for large alkenes) primary products. Note that the secondary oxidation pathways for both the dienedial and the epoxide are expected to produce both glyoxal and methylglyoxal. This secondary oxidation hypothesis would simultaneously explain why the dienedial and epoxide primary oxidation products have often not been observed at the same time that relatively high yields of glyoxal and methylglyoxal have been observed. As discussed

in detail above, our experimental method differs from many of the previous methods in that it is capable of confining the fate of OH radicals almost exclusively to reaction with toluene, and not to reaction with primary oxidation products. On the basis of our primary oxidation yield measurements of $23.5 \pm 8.7\%$ dienedial and $7.2 \pm 2.5\%$ epoxide, we predict that the maximum glyoxal and methylglyoxal secondary oxidation yield should be on the order of $30 \pm 10\%$. Therefore, depending on the importance of secondary oxidation processes in the previous experiments, glyoxal and methylglyoxal yields between 0 and 40% are consistent with the present results. This estimate is consistent with the entire range of previous results reported in Table 2.

In addition, the fact that the OH-addition products (cresol, dienedial, and epoxide) were not found to be directly dependent on NO concentrations and the fact that glyoxal and methylglyoxal production was not observed in the presence of NO suggests that the NO-dependent pathways depicted in Figure 1 are not actually operative in the toluene primary oxidation system. Furthermore, it is proposed that the NO-dependence observed in previous measurements is due to the role of NO in converting the HO₂ product that is produced by most of the primary oxidation pathways into OH (which helps to initiate the secondary oxidation processes depicted in Figure 4), and the role that NO directly plays in the secondary oxidation mechanisms.

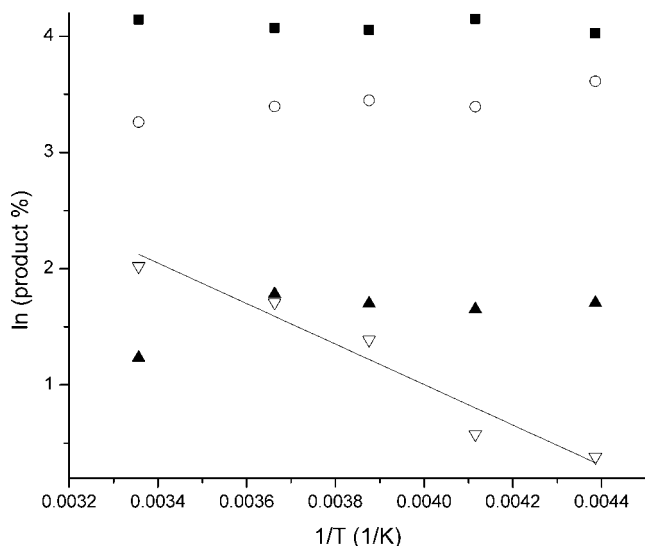


Figure 5. Arrhenius analysis for the temperature dependence of the primary product yields (closed squares, cresol; open circles, dienedial; closed triangles, epoxide; open triangles, benzaldehyde).

Temperature Dependent Relative Primary Oxidation Product Yield Measurements. Because the CIMS method for the detection of toluene was much less sensitive at temperatures below 298 K, it was not possible to determine the amount of toluene reacted in the low temperature experiments. Therefore, only relative product yields could be determined at these lower temperatures. Figure 5 shows an Arrhenius analysis for the temperature dependence (228–298 K) of the relative product yields for the benzaldehyde, cresol, dienedial, and the epoxide primary products. All three OH-addition channel products show no statistically significant temperature dependence, while the OH-abstraction channel product benzaldehyde shows strong positive Arrhenius behavior, with an effective activation energy of 14 ± 2 (1σ) kJ/mol. Although there are several processes that lead to the production of these primary products, each with its own temperature dependence, the present results are consistent with the initial OH reaction as the controlling factor in the overall temperature dependence of the product yields: addition reactions are often observed to follow small, negative Arrhenius behavior, while abstraction reactions are often observed to follow large, positive Arrhenius behavior. For example, the activation energies for OH-abstraction reactions involving alkanes are on the order of 10 kJ/mol,²⁹ a value similar to that determined here. An earlier study investigated the o-cresol and benzaldehyde yields from toluene and found them to be temperature independent over a modest range of temperatures (303–323 K).²⁶ In any case, with the exception of the relatively minor product benzaldehyde, the primary product yields do not appear to depend strongly on temperature over tropospherically relevant temperatures.

Atmospheric Implications. The present determination of a major primary product oxidation pathway involving the formation of a dienedial product and OH suggests that a significant fraction of atmospheric primary toluene oxidation may be characterized by a null cycle with respect to ozone formation chemistry. Obviously, this outcome would provide one possible explanation (another possible explanation is that the secondary chemistry is incorrect) for the environmental chamber modeling experiments that suggest that the MCM model (which does not have any dienedial chemistry) overpredicts ozone production and underpredicts OH levels in toluene oxidation systems representative of the atmosphere.⁴ In addition, the

present observation that dienedial and epoxide products are major primary oxidation products for toluene and that glyoxal and methylglyoxal are not major primary oxidation products suggests that previous experiments in which glyoxal and methylglyoxal are observed were likely operating under conditions of significant secondary oxidation of the primary dienedial and epoxide products. In summary, the present results suggest that the MCM model for toluene oxidation should be modified to more accurately represent the primary and secondary oxidation chemistry, which will likely lead to new conclusions concerning the role of toluene in the atmospheric formation of ozone and SOA.

Acknowledgment. This material is based upon work supported by the National Science Foundation under Grant No. 0753103 and a Henry Dreyfus Teacher-Scholar Award.

References and Notes

- (1) In *Chemistry of atmospheres*; Wayne, R. P., Ed.; Oxford University Press: Oxford, U.K., 2000.
- (2) In *The mechanisms of atmospheric oxidation of aromatic hydrocarbons*; Calvert, J. G., Atkinson, R., Becker, K. H., Kamens, R. M., Seinfeld, J. H., Wallington, T. J., Yarwood, G., Eds.; Oxford University Press: Oxford, U.K., 2002.
- (3) Offenberg, J. H.; Lewis, C. W.; Lewandowski, M.; Jaoui, M.; Kleindienst, T. E.; Edney, E. O. *Environ. Sci. Technol.* **2007**, *41*, 3972.
- (4) Wagner, V.; Jenkin, M. E.; Saunders, S. M.; Stanton, J.; Wirtz, K.; Pilling, M. J. *Atmos. Chem. Phys.* **2003**, *3*, 89.
- (5) Bloss, C.; Wagner, V.; Jenkin, M. E.; Volkamer, R.; Bloss, W. J.; Lee, J. D.; Heard, D. E.; Wirtz, K.; Martin-Reviejo, M.; Rea, G.; Wenger, J. C.; Pilling, M. J. *Atmos. Chem. Phys.* **2005**, *5*, 641.
- (6) Klotz, B. G.; Bierbach, A.; Barnes, I.; Becker, K. H. *Environ. Sci. Technol.* **1995**, *29*, 2322.
- (7) Volkamer, R.; Platt, U.; Wirtz, K. *J. Phys. Chem. A* **2001**, *105*, 7865.
- (8) Kroll, J. H.; Ng, N. L.; Murphy, S. M.; Varutbangkul, V.; Flagan, R.; Seinfeld, J. H. *J. Geophys. Res.* **2005**, (D23207), 1.
- (9) Forstner, H. J. L.; Flagan, R. C.; Seinfeld, J. H. *Environ. Sci. Technol.* **1997**, *31*, 1345.
- (10) Hamilton, J. F.; Webb, P. J.; Lewis, A. C.; Reviejo, M. M. *Atmos. Environ.* **2005**, *39*, 7263.
- (11) Klotz, B.; Volkamer, R.; Hurley, M. D.; Andersen, M. P. S.; Nielsen, O. J.; Barnes, I.; Imamura, T.; Wirtz, K.; Becker, K. H.; Platt, U.; Wallington, T. J.; Washida, N. *Phys. Chem. Chem. Phys.* **2002**, *4*, 4399.
- (12) Berndt, T.; Boge, O. *Phys. Chem. Chem. Phys.* **2001**, *3*, 4946.
- (13) Moschonas, N.; Danalatos, D.; Glavas, S. *Atmos. Environ.* **1999**, *33*, 111.
- (14) Klotz, B.; Sorensen, S.; Barnes, I.; Becker, K. H. *J. Phys. Chem. A* **1998**, *102*, 10289.
- (15) Smith, D. F.; McIver, C. D.; Kleindienst, T. E. *J. Atmos. Chem.* **1998**, *30*, 209.
- (16) Becker, K. H.; Barnes, I.; Bierbach, A.; Brockmann, K. J.; Kirchner, F. *Chemical processes in atmospheric oxidation*; Springer-Verlag: Berlin, 1997; pp 79–90.
- (17) Seuwen, R.; Warneck, P. *Int. J. Chem. Kinet* **1996**, *28*, 315.
- (18) Atkinson, R.; Arey, J.; Tuazon, E. C.; Aschmann, S. M.; Bridier, I., Experimental investigation of the Atmospheric Chemistry of Aromatic Hydrocarbons and Long-Chain Alkanes (ARB-R-94/550; Order No. PB95 109591); Statewide Air Pollution Res. Cent., California Univ.: Riverside, CA, 1994.
- (19) Atkinson, R.; Aschmann, S. M.; Arey, J.; Carter, W. P. L. *Int. J. Chem. Kinet* **1989**, *21*, 801.
- (20) Dumdei, B. E.; Kenny, D. V.; Shepson, P. B.; Kleindienst, T. E. *Environ. Sci. Technol.* **1988**, *22*, 383.
- (21) Tuazon, E. C.; MacLeod, H.; Atkinson, R.; Carter, W. P. L. *Environ. Sci. Technol.* **1986**, *20*, 383.
- (22) Gery, M. W.; Fox, D. L.; Jeffries, H. E.; Stockburger, L.; Weathers, W. S. *Int. J. Chem. Kinet* **1985**, *17*, 931.
- (23) Bandow, H.; Washida, N.; Akimoto, H. *Bull. Chem. Soc. Jpn.* **1985**, *58*, 2531.
- (24) Shepson, P. B.; Edney, E. O.; Corse, E. W. *J. Phys. Chem.* **1984**, *88*, 4122.
- (25) Tuazon, E. C.; Atkinson, R.; MacLeod, H.; Biermann, H. W.; Winer, A. M.; Carter, W. P. L.; Pitts, J. N., Jr. *Environ. Sci. Technol.* **1984**, *18*, 981.
- (26) Atkinson, R.; Carter, W. P. L.; Winer, A. M. *J. Phys. Chem.* **1983**, *87*, 1605.
- (27) Yu, J.; Jeffries, H. E. *Atmos. Environ.* **1997**, *31*, 2281.

- (28) Miller, A. M.; Yeung, L. Y.; Kiep, A. C.; Elrod, M. J. *Phys. Chem. Chem. Phys.* **2004**, *6*, 3402.
- (29) NIST Chemical Kinetics Database, <http://kinetics.nist.gov/kinetics/index.jsp>, accessed September 2008.
- (30) Fritz, J. J.; Fuget, C. R. *Chem. Eng. Data Ser.* **1956**, *1*, 10.
- (31) Bohn, B. J. *Phys. Chem. A* **2001**, *105*, 6092.
- (32) Spanel, P.; Smith, D. *Int. J. Mass Spectrom.* **1997**, *167*, 375.
- (33) Spanel, P.; Doren, J. M. V.; Smith, D. *Int. J. Mass. Spectrom.* **2002**, *213*, 163.
- (34) Spanel, P.; Wang, T.; Smith, D. *Int. J. Mass Spectrom.* **2002**, *218*, 227.
- (35) Messer, B. M.; Stielstra, D. E.; Cappa, C. D.; Scholtens, K. W.; Elrod, M. J. *Int. J. Mass Spectrom.* **2000**, *197*, 219.
- (36) Ranschaert, D. L.; Schneider, N. J.; Elrod, M. J. *J. Phys. Chem. A* **2000**, *104*, 5758.
- (37) Elrod, M. J.; Ranschaert, D. L.; Schneider, N. J. *Int. J. Chem. Kinet* **2001**, *33*, 363.
- (38) Chow, J. M.; Miller, A. M.; Elrod, M. J. *J. Phys. Chem. A* **2003**, *107*, 3040.
- (39) Yeung, L. Y.; Pennino, M. J.; Miller, A. M.; Elrod, M. J. *J. Phys. Chem. A* **2005**, *109*, 1879.
- (40) Patchen, A. K.; Pennino, M. J.; Elrod, M. J. *J. Phys. Chem. A* **2005**, *109*, 5865.
- (41) Hsin, H. Y.; Elrod, M. J. *J. Phys. Chem. A* **2007**, *111*, 613.

JP806841T